Total Ozone Determination from the Backscattered Ultraviolet (BUV) Experiment

K. F. KLENK,* P. K. BHARTIA,* A. J. FLEIG,† V. G. KAVEESHWAR,*
R. D. MCPETERS* AND P. M. SMITH*,[1]

*Systems and Applied Sciences Corporation, Riverdale, MD 20737,
†NASA Goddard Space Flight Center, Greenbelt, MD 20770

(Manuscript received 13 February 1982, in final form 18 July 1982)

ABSTRACT

The algorithm used to derive total ozone from the Nimbus 4 Backscattered Ultraviolet (BUV) experiment is described. A seven-year global data set with more than one million retrievals has been produced and archived using this algorithm. The algorithm is a physical retrieval scheme using accurate radiative transfer computations. Error sources are discussed and verified using Dobson network comparisons and the statistics of the BUV A- and B-pair derived ozone values.

1. Introduction

Dave and Mateer (1967) demonstrated the feasibility of determining atmospheric ozone from measurements of the backscattered solar ultraviolet radiation at wavelengths near 310 nm. This was the basis of the algorithm later developed by Mateer *et al.* (1971) and used to obtain total ozone from measurements of UV radiances from the Backscatter Ultraviolet (BUV) experiment (Heath *et al.*, 1970) on the Nimbus 4 satellite for the initial months of operation. In 1976, NASA established the Ozone Processing Team (OPT) to create an extended multi-year BUV total ozone and ozone vertical profile data set. The original total ozone algorithm was critically evaluated and modifications were made, based on the results of error studies and instrument performance evaluations. This paper describes the operational total ozone algorithm used to process the BUV total ozone data, archived in the National Space Science Data Center (World Data Center-A for Rockets and Satellites), in November 1979.

The BUV experiment measures both the solar radiation backscattered by the earth and the solar irradiance in 12 wavelength bands, 1.0 nm wide, between 255.5 and 339.8 nm. Solar irradiance is measured by deploying a diffuser plate. The four longest bands centered at 312.5, 317.5, 331.2 and 339.8 nm are used by the total O_3 algorithm. The band centers and corresponding scattering and absorption coefficients are given in Table 1. Simultaneous measurements outside the O_3 absorption band are made at 380 nm with a filter photometer. Both the photometer and the monochromator have a 200 km square field of view (FOV) at the earth's surface.

The solar irradiance measurement was made by deploying a diffuser plate in the instrument's FOV to reflect the solar radiation. Unfortunately, the reflecting properties of the diffuser plate changed dramatically with time, making the determination of any time dependence in the solar flux impossible. Time-independent values of the solar flux were used in the processing of the BUV data. The solar flux values were obtained by extrapolating the observed output to the first day of BUV operation.

2. Theoretical foundation

The backscattered radiance I is a function of many variables. The most important variables for the ozone algorithm are symbolized in the following expression:[2]

$$\frac{I}{F} = f(\lambda, \theta_0, \Omega, R, P_0, \mathcal{S}), \tag{1}$$

where:

- λ wavelength
- θ_0 solar zenith angle
- Ω total ozone amount in a vertical column of unit area
- R surface reflectivity

[1] Present affiliation: NASA Goddard Space Flight Center, Greenbelt, MD 20770.

[2] Rigorously, the radiance depends on the ozone density as a function of atmospheric pressure. Thus Eq. (1) should be written as $I/F = f(\lambda, \theta_0, R, P_0, X(p))$. However, for the total ozone wavelengths and for solar zenith angles less than 80° the backscattered radiance is only weakly dependent on the distribution of the stratospheric profile. Eq. (1) represents the stronger dependence on total ozone and the much weaker dependence on profile shape written symbolically as $\mathcal{S}$.

0021-8952/82/111672-13$07.25

TABLE 1. BUV scattering and absorption coefficients.

Wavelength* (nm)	Scattering coefficient (atm^{-1})**	Absorption coefficients ($atm\text{-}cm^{-1}$)
312.60	1.023	0.710
317.63	0.956	0.392
331.29	0.799	0.074
339.93	0.717	0.018
380.	0.450	0.

* In air.
** 1.0 atm = 1.01325×10^5 Pa.

p_0 surface pressure
$\mathscr{S}$ a symbol denoting the dependence on ozone profile shape
F extraterrestrial solar flux.

The wavelength λ and the solar zenith angle θ_0 are known for each measurement. In order to obtain total ozone, R, p_0 and $\mathscr{S}$ need to be specified.

The radiance I (for $\lambda > 310$ nm) consists primarily of solar radiation which penetrates the stratosphere. The radiation is reflected by the dense tropospheric air, clouds and the surface. The reflecting surface and almost 90% of the scattering atmosphere lie below the tropopause, above which lies almost 90% of the atmospheric ozone. Total O_3 retrieval without knowledge of the vertical distribution of the O_3 is possible because of the nearly complete spatial separation of the absorbers (i.e., the ozone molecules) from the scatterers and reflectors. The O_3 acts as an attenuator of the direct solar flux going to the troposphere and of the diffuse radiation scattered and reflected from it. Thus, the dependence on the distribution of O_3 is weak at all angles, except at very large solar zenith angles where the radiation does not effectively penetrate to the troposphere. The separation of the absorbers from the scatterers makes it possible to redefine R to include the effect of clouds and aerosols. From an analysis of the studies of Dave (1978) on the effect of aerosols on the backscattered radiance, and of Fraser and Ahmad (1978) on the effect of clouds and sea glint on the total ozone determination, we found that the radiative properties of aerosols, clouds and sea glint need not be explicitly included in the algorithm. It is possible to account for these effects by replacing the true surface reflectivity in Eq. (1) with an effective surface reflectivity of generally higher value derived from the radiance measurement outside the O_3 absorption band.

For a Lambertian reflecting surface, the reflectivity R can be separated from the functional form given in Eq. (1). Dave (1964) has shown that the total backscattered intensity I can be expressed as a sum of two terms: a purely atmospheric backscattered intensity I_0 which is unaffected by the surface; and a component which accounts for the direct and the diffuse radiation reflected by the surface:

$$I(\lambda, \theta_0, \Omega, R, p_0, \mathscr{S}) = I_0(\lambda, \theta_0, \Omega, p_0, \mathscr{S}) + \frac{R \cdot T(\lambda, \theta_0, \Omega, p_0, \mathscr{S})}{1 - RS_b(\lambda, \Omega, p_0, \mathscr{S})}. \quad (2)$$

Here T is the total amount of direct plus diffuse radiation reaching the surface, multiplied by the atmospheric transmission of the diffuse reflected radiation in the direction of the satellite. T includes both directly transmitted and air-scattered radiation emerging at the top of the atmosphere. The numerator in the second term on the right-hand side accounts for the once-reflected radiation. Multiple reflection by the surface is accounted for by the term in the denominator, where S_b is the fraction of the reflected radiation, scattered back to the surface by the atmosphere.

For a wavelength outside the O_3 absorption band (380 nm), the radiance is ozone independent and does not depend on Ω and $\mathscr{S}$. Therefore, Eq. (2) can be inverted to compute the effective surface reflectivity R once the surface pressure p_0 is known.

The pressure p_0 of the effective Lambertian surface is not directly retrievable from the BUV radiances. For scenes not covered with clouds, the pressure can be obtained from standard terrain height tables. Ideally, in the presence of clouds, one needs a simultaneous independent measurement of the cloud top height. Lacking this information, the algorithm estimates the effective surface pressure from the reflectivity and latitude as described in Section 3d.

3. The total ozone algorithm

Total ozone is obtained by matching the measured radiances with computed radiances in a look-up table. The computation of the radiance look-up tables is described in Section 3a. The scene reflectance is determined by using the photometer measurements at 380 nm where there is no absorption by ozone (see Section 3b). Values of total ozone at two surface pressures are determined by using the derived reflectance and the four longest monochromator radiances (Section 3c). The recommended value of ozone is based on the estimated pressure of the reflecting surface (Section 3d), and also on the latitude and a weighted mix of the two pair-ozone values based on the solar zenith angle of the observation (Section 3e). Finally (Section 3f), we describe several validity checks which are used to maintain data quality.

a. *Computation of theoretical radiances*

Tables of the nadir backscattered radiance are required for each wavelength band and for several values of solar zenith angle θ_0, surface reflectivity R and pressure p_0, and vertical profiles having different integrated total ozone amounts. In the ultraviolet, the incoming solar radiation is strongly multiply scattered, and the backscattered radiation is a complex function of the parameters listed above. The backscattered radiances are computed for an atmosphere containing only air and ozone with an underlying reflecting surface. The radiances are computed using the auxiliary equation solution to the radiative transfer equations developed by Dave (1964). Following Dave, multiple scattering to seven orders of scattering is computed and a geometrical series extrapolation is used to approximate the remaining very small contribution for higher orders. The classical Rayleigh phase matrix is used and full account of polarization is taken. The band-scattering coefficients are based on the Penndorf (1957) tables. The reflecting surface is assumed to be Lambertian. Sphericity of the earth's atmosphere is accounted for accurately (DeLuisi and Mateer, 1971) for the primary scattering, but higher orders of scattering are calculated, assuming a plane-parallel atmosphere. The O_3 absorption coefficients are based on the −44°C measurements of Vigroux (1953). Klenk (1980) has described the computation of effective absorption and scattering coefficients for the BUV wavelength bands.

A set of 21 standard climatological O_3 vertical profiles[3] are used to account for the dependence of the radiances on total ozone Ω and profile shape $\mathcal{S}$. The profiles were constructed from a large number of ozonesonde measurements which were averaged according to total O_3 and latitude band. There are significant differences in shape between profiles having the same O_3 amount but corresponding to different latitude bands. Three such profiles containing a total O_3 of 0.300 atm-cm are shown in Fig. 1. For the purpose of total O_3 computation, the important difference between these profiles is the shifting of the ozone density maximum to lower altitudes in going from low to high latitudes. The standard profiles account for the systematic latitudinal variation in the vertical ozone distribution below 40 km. There are three low-latitude profiles corresponding to O_3 amounts of 0.20 to 0.30 atm-cm, eight midlatitude profiles corresponding to amounts from 0.20 to 0.55 atm-cm, and ten high latitude profiles corresponding to amounts from 0.20 to 0.65 atm-cm, all in 0.05 atm-cm increments. The total O_3 represents the integrated ozone amount from outside the atmosphere, to an atmospheric pressure of 1.0 atm. The increasing range in ozone from the low to high latitude bands reflects the pattern of the natural variability of ozone, which is relatively constant in the equatorial regions and more highly variable in the higher latitudes.

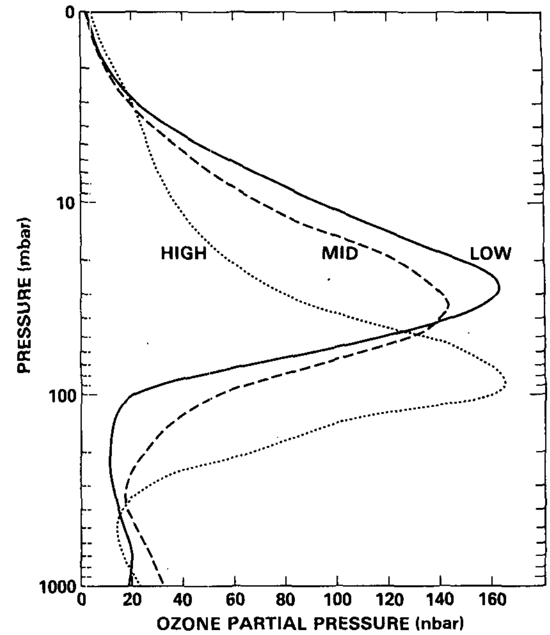

FIG. 1. Ozone vertical profiles for the low, middle and high latitudes each corresponding to a total ozone amount of 0.3 atm-cm.

The radiance tables consist of several smaller tables representing the three functions I_0, T and S_b, appearing in Eq. (2). For the monochromator bands (λ = 312.5, 317.5, 331.2 and 339.8 nm), I_0 and T are tabulated for 10 values of θ_0,[4] two values of the surface pressure,[5] and for the 21 standard profiles; and S_b is tabulated for the two values of the surface pressure and for each of the 21 standard profiles. For the photometer band (λ = 380 nm), I_0 and T are tabulated for the 10 values of θ_0 and two values of surface pressure; and S_b is tabulated for the two values of surface pressure.

b. *Computation of reflectivity*

The effective reflectivity is computed from the measured photometer radiance I_{380} by solving Eq. (2) to obtain

$$R = \frac{I_{380} - I_0(380, \theta_0, p_0)}{T(380, \theta_0, p_0) + s_b(380, p_0)} \times [I_{380} - I_0(380, \theta_0, p_0)]. \quad (3)$$

The BUV monochromator steps through the 12

[3] A set of over 6000 ozone profiles measured by balloonborne instruments were categorized according to latitude and total ozone amount. Three latitude ranges, ±25°, ±25° to ±55° and poleward of 55°, and 0.05 m-atm-cm bins of total ozone were used. Rocket soundings were averaged by latitude to determine the upper-level profile (40–1 mb). The average profiles were computed by E. Hilsenrath, P. Dunn and C. Mateer and were presented at the IAGA/IAMAP Joint Assembly in Seattle, Washington, August 1970. The standard ozone profiles were derived from these averaged profiles by C. Mateer.

[4] In degrees: 0, 33.7, 48.4, 60.3, 71.1, 77.1, 80.4, 82.7, 84.4 and 85.7.

[5] 0.4 and 1.0 atm.

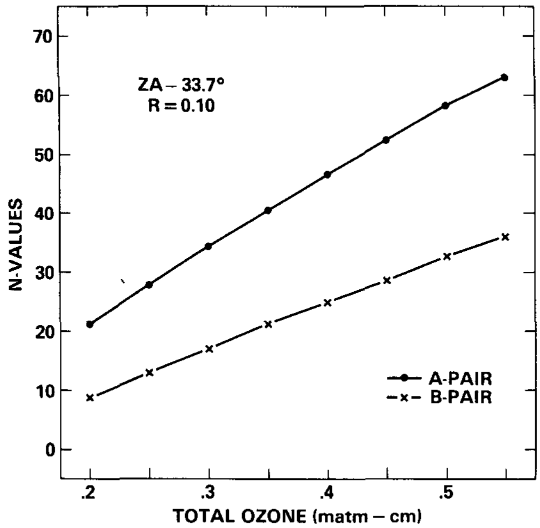

FIG. 2. N–Ω curve for A- and B-pairs for a solar zenith angle (ZA) of 33.7° and a surface reflectivity (R) of 0.1.

wavelength bands sequentially in 1.5 steps. Since the FOV of the instrument changes by ~3% every second, due to the satellite motion, significant scene changes can occur in the time it takes the instrument to step through the four total ozone bands. To account for this effect, photometer measurements are made simultaneously with each of the monochromator steps. Thus, four values of the photometer reflectivity are computed corresponding to the four total ozone FOV's. Since the surface pressure in the FOV is not known at this stage of computation, reflectivities are computed using both 1.0 and 0.4 atm tables.

c. Computation of total ozone

To compute total ozone, measured radiances are paired in a manner similar to the ground based Dobson (Dobson, 1963) and Umkehr (Mateer and Dutsch, 1964) experiments. A longer wavelength measurement, which is relatively insensitive to O_3, is paired with an ozone-sensitive wavelength, primarily to eliminate errors due to absolute uncertainties in the monochromator calibration. Two wavelength pairs are used in this algorithm: the A-pair, composed of the 312.5 and 331.2 nm bands and the B-pair, composed of the 317.5 and 339.8 nm bands.

The dependence of the backscattered radiance on O_3 is approximately exponential. A quantity called the N-value is defined to reduce the dynamic range of the total O_3 dependence. The N_λ-value for a wavelength band is defined as

$$N_\lambda = -100 \log_{10} \frac{I_\lambda}{F_\lambda}, \tag{4}$$

and for a wavelength pair as

$$N_{\text{pair}} = N_\lambda - N_{\lambda'} = -100 \log_{10}\left[\left(\frac{I_\lambda}{F_\lambda}\right)\Big/\left(\frac{I_{\lambda'}}{F_{\lambda'}}\right)\right]. \tag{5}$$

To determine total ozone, the following procedure is used. The N_{pair} versus total O_3 dependence is constructed for each pair from the radiance tables using Eqs. (2), (4) and (5), the values of R obtained from the photometer radiances, and values of T and I_0 interpolated to the solar zenith angle of the scene being measured. This dependence is illustrated in Fig. 2, for a reflectance of 0.1, solar zenith angle of 33.7° and middle latitudes. The N_{pair} values are joined to obtain a piecewise linear curve. Total O_3 for each pair is obtained by linear interpolation between adjacent points using the measured value of N_{pair}.

For each retrieval, the algorithm derives O_3 values independently from the two pressure tables for the appropriate latitude band and for both the A and B wavelength pairs. Thus, four O_3 values are computed. In latitude bands which form boundaries for the low and middle, and middle and high latitudes, ozone values are derived for both of the two appropriate latitude bands. The first step to obtain a single "best" ozone is to determine the effective pressure or height which is assigned to the reflecting surface.

d. Determination of surface pressure

No direct measure of reflecting surface pressure is available from the BUV instrument. Instead, the pressure level is inferred from the measured reflectivity. The assumption is that clouds are good reflectors of UV radiation while land and sea are poor reflectors. Thus, if the effective reflectivity is large ($R > 0.6$), it is assumed the reflection is from clouds. If the reflectivity is low ($R < 0.2$), reflection from the surface is assumed. In the absence of definitive cloud statistics, we have assumed that whenever there are clouds, the cloud top pressure is 0.4 atm. The surface pressure used is based on a terrain height tape obtained from NOAA. Terrain height averaged over 2° × 2° areas is stored in tables as a function of latitude and longitude. The 1976 Standard Atmosphere (COESA, 1976) pressure-height relationship is used to convert this terrain height to a terrain height pressure P_{terrain}. Intermediate reflectivities ($0.2 < R < 0.6$) are assumed to be from partly cloudy scenes. A reflectivity weighted pressure is determined from the surface and cloud top heights as

$$P = [(0.6 - R)P_{\text{terrain}} + (R - 0.2)(0.4 \text{ atm})]/0.4. \tag{6}$$

A complication to this scheme for assigning reflecting surface pressure is that it is possible for the surface to be covered by snow or ice and have a very high reflectivity but be close to sea level. The reflectivities derived from BUV over permanently snow-covered regions such as Greenland and Antarctica are invariably higher than the maximum reflectivities

($R \approx 0.8$) observed in lower latitudes. Since there is no way to differentiate between snow/ice and clouds over snow/ice, the following adjustment is made for latitudes poleward of 55°. For $R > 0.8$, a mix of the terrain height pressure and the nominal cloud pressure (0.4 atm) is applied with weights of 3 to 1:

$$P = \tfrac{3}{4}P_{\text{terrain}} + \tfrac{1}{4}(0.4 \text{ atm}). \tag{7}$$

For $0.6 < R < 0.8$, and latitudes greater than 55° the pressure is assumed to increase linearly from 0.4 atm at $R = 0.6$ to the pressure given in Eq. (7) at $R = 0.8$.

e. Best ozone determination

Having determined an effective surface pressure, the corresponding ozone amount for each pair is computed by linear interpolation of the ozone derived using the 1.0 and 0.4 atm tables.[6]

In generating the 0.4 atm tables, the ozone contained in the climatological profiles below 0.4 atm has no effect on the computed backscattered radiance since the reflecting surface is assumed to be opaque. However, the ozone below 0.4 atm is included in the total ozone amount, when the 0.4 tables are used in order to account, albeit climatologically, for the ozone amount below the cloud. For elevated terrain, the amount of O_3 in the climatological profile below the pressure corresponding to the terrain is not included in the derived total O_3.

The climatological profiles used to generate the standard radiance tables exhibit significant differences among the three latitude types, i.e., low, middle and high latitude types. We have defined boundary regions in which a shift from one latitude zone to a neighboring latitude is made. These latitude boundary regions are:

20–30° for low/middle zones

50–60° for middle/high zones.

The derived total O_3 for a latitude lying in one of these boundary regions is a linear mix of the total O_3 values derived from the standard tables for the two neighboring zones. For example, if the latitude L is between 50 and 60°, the latitude mix gives

$$\Omega = \tfrac{1}{10}[(60 - L)\Omega_{\text{mid}} + (L - 50)\Omega_{\text{high}}], \tag{8}$$

where Ω_{mid} and Ω_{high} are the pressure mixed middle latitude and high latitude values, respectively. One such value is obtained for each of the two pairs.

The relative sensitivity of the A- and B-pair N-values to total O_3 varies significantly with solar zenith angle. Referring to Fig. 2, it can be seen that for near overhead sun conditions, the A-pair is more sensitive (~1.6 times) to ozone than the B-pair. As a result, the B-pair ozone is found to be affected more by uncertainties in instrument calibration and errors in modeling the atmosphere. This situation reverses as we approach the solar terminator. The A-pair loses its sensitivity to total O_3 because the 312.5 nm radiance no longer effectively penetrates to the atmosphere below the O_3 maximum. On the other hand, the 317.5 nm radiances penetrate deeper into the atmosphere; hence, the B-pair loses its sensitivity much more slowly. This effect can be seen in Fig. 3, which shows the N–Ω curves for low sun conditions, $\theta_0 = 80.4°$. The difference in the height of the scattering layer between 312.5 and 317.5 nm wavelengths implies that the A-pair radiances are more sensitive to the O_3 profile shape than the B-pair. If the actual profile shape differs substantially from the climatological profile, the A-pair O_3 will be more in error at large solar zenith angles than the B-pair O_3 values.

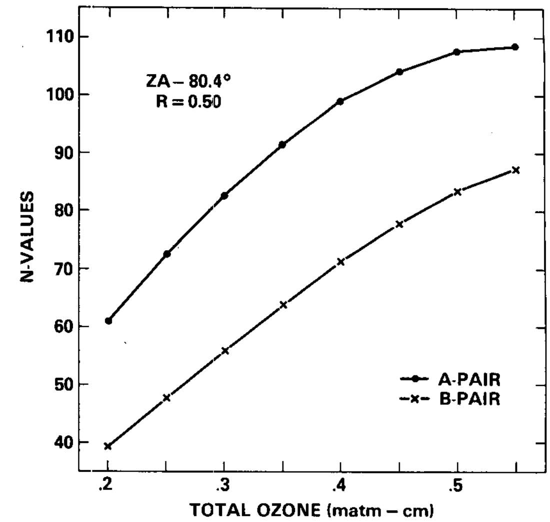

FIG. 3. N–Ω curve for A- and B-pairs for a solar zenith angle (ZA) of 80.4° and a surface reflectivity (R) of 0.5.

In order to optimize the retrieval accuracy under all sun conditions, A- and B-pair ozone amounts are combined into a single recommended or "best" ozone value. The relative weighting of the pairs is done such that the A-pair answer is chosen at low solar zenith angles and the B-pair answer is chosen at large zenith angles. At intermediate solar zenith angles, a smooth transition is made from the A-pair to B-pair result. The best ozone is given by

$$\Omega_{\text{best}} = \Omega_{\text{A}} W + \Omega_{\text{B}}(1 - W). \tag{9}$$

In this equation, Ω_{A} and Ω_{B} are the pressure and latitude mixed ozone amounts and the weight W is a function of the slant path S $(= 1 + \sec\theta_0)$ as follows:

[6] The linear approximation has been tested by comparing interpolated values to values obtained by solution of the radiative transfer equation. The pressure interpolation was found to be accurate to within 1%.

$$W = \begin{cases} 1, & S \leqslant 2.2 \quad (\theta_0 \leqslant 37^\circ) \\ \dfrac{S-5}{2.85}, & 2.2 < S < 5.0 \quad (37^\circ < \theta_0 < 76.3^\circ). \\ 0, & S \geqslant 5.0 \quad (\theta_0 \geqslant 76.3^\circ) \end{cases} \tag{10}$$

This procedure of mixing the ozone derived from the two pairs assumes that A- and B-pair estimates have the same mean value. However, from an analysis of the Nimbus 4 BUV total ozone data, it was found that the A-pair ozone was consistently higher than the B-pair ozone by $\sim$3.5% when using the Vigroux (1953) ozone spectrum. This bias between the pairs would result in an artificial latitudinal dependence of the best ozone. The most likely cause for such a systematic bias between the two pairs is inconsistency of the O_3 absorption coefficients. Klenk (1980) has shown that the different laboratory experiments consistently agree at 317.5 nm, but vary considerably at 312.5 nm. Consequently, we adjusted the A-pair for the bias in obtaining the best O_3 as follows:

$$\Omega_{\text{best}} = 0.965 W\Omega_A + (1 - W)\Omega_B ,$$

where Ω_A, Ω_B and W are as defined above. This adjusted result is very nearly the result we would have obtained using the Inn and Tanaka (1959) spectrum, corrected to the nominal stratospheric temperature of -44°C.

f. Validity checks

The algorithm contains validity checks to maintain data quality. In processing prior to O_3 determination, checks are made on the solar zenith angle, satellite attitude, instrument status and instrument output. This section describes the quality checks performed on the derived reflectivity and O_3. The purpose of these checks is to identify bad scans due to bad input which passes preprocessing checks or to limitations of the ozone algorithm.

Computed total O_3 for each pair must be within the range of the radiance tables. For low, middle and high latitudes, the total O_3 ranges are 0.18–0.32, 0.18–0.55 and 0.18–0.65 atm-cm, respectively. When the pair ozone exceeds the range, an error in the input data is usually the cause. When this occurs, that affected pair ozone value is not reported and no best ozone is recommended.

The sensitivity of the B-pair N-value to total ozone must be greater than 20 atm-cm^{-1} (i.e., the N-value must vary by more than 1 unit for a 0.05 atm-cm change in ozone). Such small values of the sensitivity occur only at large solar zenith angles. Ozone values derived from portions of the radiance table where there is little or no dependence on ozone are extremely error prone and are rejected.

Reflectivity derived using the 380.0 nm photometer and 339.8 nm monochromator channels are compared. No best ozone is computed when the reflectivities differ by more than 0.1. Such large differences occur infrequently and are due to malfunctions in the instrument performance of either the photometer or the monochromator or in the recording or transmission of the data.

A check is made on the difference between the A-pair and B-pair ozone. If the difference exceeds 10% of the best ozone, then the best ozone is flagged but not deleted. This check is particularly important at large solar zenith angles where A − B differences are indicative of substantial profile shape departures from the algorithmic models. This check preferentially edits retrievals at larger values of total ozone, since the errors increase for the A-pair with increased O_3 amount. Zonal means computed without the O_3 values flagged for AB difference will be underestimates of the true zonal mean. Therefore, we recommend using these flagged values in the computation of zonal means.

4. Analysis of errors

The seemingly simple question, "What is the error in the BUV total ozone measurement?", does not have a simple answer. Error sources are many and varied in nature. Furthermore, the importance of a particular error to a user of the data will depend on what he needs the data for. Some users of total O_3 will be interested in the precision of the data. Others may be interested in the absolute accuracy of the retrieval or in those errors causing artificial long-term changes in O_3. Further complicating the answer to "what is the error?" is the fact that the dominant error in an individual retrieval is dependent on the observational situation. This is because the algorithmic errors and measurement errors propagate differently, depending on solar zenith angle, surface reflectivity, whether the A- or B-pair is used, presence of clouds, etc.

We have made an extensive study of the errors in BUV total O_3 retrieval. In this section we will present an overview of the BUV errors. This error analysis is based on our best estimation of the errors in calibration, algorithm modeling and in external independent information used as input to the algorithm. Many of the important derived errors have been verified by comparison with Dobson total ozone data and by internal consistency analysis of the BUV data alone. (The observed errors will be discussed in Section 6.)

a. Ozone absorption coefficients

Many authors (Inn and Tanaka 1959; DeLuisi 1975; Klenk 1980; Komhyr 1980) have pointed out that there are significant discrepancies among the various laboratory and atmospheric measurements of the O_3 absorption coefficients. Klenk has shown that atmospheric measurements of total O_3 using Dobson AD and CD, and BUV A and B wavelength pairs derived with the Inn and Tanaka (1959) spectrum have inconsistencies of 4%. The use of other laboratory spectra lead to larger errors.

DeLuisi (1980) has compared ozone retrievals using detailed spectral measurements with those based on the AD pair wavelengths. He found an average difference of 6% between the two approaches when using the Vigroux (1953) spectrum. Recent high-resolution measurements by McPeters and Bass (1982) reduce the inconsistency of the atmospheric total ozone observation of Dobson and BUV to ~2%. For the BUV and Dobson data sets, the ozone absorption coefficients may introduce bias errors of up to 6% in the total ozone. An accuracy of approximately 3% is attainable with the Bass coefficients.

b. Tropospheric ozone variability

Ozone in the lowest few kilometers of the atmosphere above the earth's surface is difficult to detect in the BUV method. When the underlying surface is dark, the algorithm will underestimate any deviations from the standard profile amount. The opposite is true when the surface is very highly reflecting. The tropospheric O_3 sensitivity dependence is illustrated in Table 2. We used a standard midlatitude profile with 350 m-atm-cm of O_3 and added 10 m-atm-cm to the lower (0–5 km) or upper (5–10 km) part of the troposphere. We then generated the radiances that would be detected for this modified profile for a range of surface reflectivities and solar zenith angles and ran these through the algorithm. Table 2 shows how much of the additional 10 m-atm-cm would be detected. For low reflecting surfaces which correspond to clear land or ocean scenes ($R \leq 0.2$), the algorithm senses only 20–66% of the added ozone. For high reflecting surfaces ($R \geq 0.8$), such as an ice surface, the added ozone amount is overestimated by up to 47% for solar zenith angles less than 60°. This case, which amounts to a fully snow-covered FOV in the equatorial region, does not actually occur. Thus, the error is nearly always one of underestimation. The second part of the table shows that the BUV measurements are much more sensitive to O_3 variations that occur in the upper troposphere. For middle and high latitudes, ~6% of the total O_3 is contained in the lowest 5 km of the atmosphere. In addition, this amount is highly variable over a local region. For middle latitudes Krueger and Minzner (1976) estimate 50% variability in this range. Combining the amount of O_3 present, the variability of this amount, and the sensitivity of the algorithm to changes in this region, we estimate a random error of up to 1.5% in

TABLE 2. Tropospheric ozone sensitivity.

θ_0	$R=$ 0	0.2	0.4	0.6	0.8	1.0
			Layer 0–5 km			
0.0	4.5	6.6	8.5	10.4	12.5	14.7
33.7	4.3	6.3	8.2	10.0	11.9	14.0
60.3	3.6	5.2	6.7	8.3	9.9	11.7
77.0	2.1	3.1	4.1	5.1	6.3	7.5
82.7	2.0	3.1	4.1	5.2	6.4	7.8
			Layer 5–10 km			
0.0	9.4	10.0	10.5	10.9	11.4	11.9
33.7	9.3	9.9	10.4	10.8	11.3	11.8
60.3	8.6	9.2	9.7	10.2	10.6	11.1
77.0	6.7	7.2	7.7	8.1	8.5	9.0
82.7	5.2	5.7	6.1	6.5	7.0	7.4

an individual retrieval, due to lack of sensitivity of the BUV technique to lower tropospheric O_3. When thick clouds cover the scene, the ozone below the cloud is not sensed by the experiment. For the average cloud top (400 mb), approximately 6% of the total ozone is masked by the cloud. Since the natural variability of the tropospheric ozone is 50%, the uncertainty in the total ozone due to this error is 3%.

For low latitudes, the tropospheric O_3 variability is much less. The standard deviation of tropospheric O_3 may be as little as 10% there (Kirchhoff *et al.*, 1981). Therefore, the above errors should be scaled down accordingly.

c. Tropospheric climatology

The average amount of tropospheric ozone in the climatology used for BUV is based on thousands of balloonsonde measurements from the 1960's through 1975. Recently, Kirchoff (1982) has pointed out that there is a large discrepancy between recent balloon measurements made at Natal and the earlier measurements there. The recent measurements give a tropospheric amount about twice the amount of earlier measurements. Whether this is due to one or the other sets of measurements being in error or to a real change in the tropospheric ozone amount is not clear. There is some evidence for a long-term change in the tropospheric ozone amount. Attsmanpacher and Hartsmanngruber (1980) have seen a long-term increase in tropospheric ozone at the Hohenpeissenberg Observatory.

An error in the average tropospheric O_3 amount used in the BUV algorithm would cause a systematic error in total O_3, because of the lack of sensitivity discussed in Section 4b. If the tropospheric O_3 amount is 50% greater than the assumed value (5–6% below 5 km), then for clear-sky situations, the error is ~1.5% over bright surfaces, −1.5% over dark surfaces, and −3% for cloud-covered scenes.

A long-term drift in the tropospheric ozone amount

TABLE 3. Total ozone precision associated with measurement precision.

θ_0 (deg)	Latitude	Total ozone (m-atm-cm)	Re-flectivity	Surface pressure (atm)	Total ozone precision (%)
0	Low	250	0.0	1.0	1.3
			1.0	0.4	1.3
60	Middle	300	0.0	1.0	1.0
			1.0	0.4	0.8
77	High	350	0.0	1.0	0.9
			1.0	0.4	0.7
85.7	High	400	0.0	1.0	1.4
			1.0	1.0	1.0

would cause an error in the derived long-term variation of the total ozone. The BUV would only detect approximately one-half of the total tropospheric change.

d. Cloud surface versus snow/ice surface

The algorithm considers all reflecting scenes with $R > 0.6$ in the low and middle latitudes to be cloud-covered scenes and scenes with $0.2 < R < 0.6$ to be partly cloudy. In winter, a snow-covered land surface on a cloudless day, which has a reflectivity of 0.2–0.6, will be mistaken for partly cloudy conditions. In such cases, the ozone will be overestimated by the algorithm by an amount varying from 0–6%. The largest error will result for scenes that are completely clear but bright ($R > 0.6$). This situation occurs rarely for latitudes below 55°.

The highest reflecting surfaces are the polar ice caps which have reflectances >0.9. These surfaces occur at high latitudes where the confusion between snow/ice and cloud causes less of a problem than for middle latitudes for several reasons: 1) the algorithm chooses an effective surface pressure at high reflectivities which is a compromise between the 1.0 and 0.4 atm pressure [see Eq. (7)], 2) the Antarctic continent is elevated terrain with surface pressures <0.9 atm and, 3) high-latitude cloud tops are generally lower than 400 mb.

e. Instrument calibration

Wavelength-independent errors in the instrument calibration cancel when pairs of wavelengths are used. Because the reflectivity R is derived using a single wavelength, it is susceptible to absolute calibration error, and errors in the reflectivity propagate into errors in the total ozone. The BUV albedo calibration accuracy is determined by the accuracy with which the solar diffuser has been calibrated, i.e., 1–2%. Propagation of this error leads to only a fraction of a percent error in total ozone.

Examination of the pre-launch calibration indicated wavelength-dependent errors on the order of 1–2% may exist. A 1% relative error between the wavelengths of a pair would lead to a systematic 1% error in the total ozone.

It is not possible to determine if any long-term change in the instrument calibration occurred. Long-term increases in the equatorial albedos were observed (Fleig *et al.*, 1981). These changes are largest at the shorter BUV wavelengths. At 339.8 nm, the total 7-year change was less than 2%, while at 255.5 nm it was 15%. (We discuss the possible BUV drifts in terms of Dobson comparisons in Section 6.)

f. Measurement noise

The precision of the BUV measured radiance is limited not by the instrument or electronics, but by the size of the data word that is transmitted from the satellite. The measured radiance is digitized by a logarithmic analog-to-digital converter. The digitized measurement is proportional to the common logarithm of the raw radiance measurement. The digitization causes a ±½ unit round-off error in the N-value as defined in Eq. (4). The standard deviation of the resulting error is =0.29. For a pair of wavelengths this error becomes 0.41. The corresponding precision in total O_3 can be computed using the sensitivities $dN/d\Omega$ from the standard radiance tables. In Table 3, we tabulate the total O_3 precision for several typical values of solar zenith angle, reflectivity, surface pressure, latitude band and total O_3. The values are computed using the expression

$$P_\Omega = \frac{100}{\Omega}\frac{d\Omega}{dN}\Delta N = \frac{41}{\Omega}\frac{d\Omega}{dN},$$

where P_Ω is the precision in the total ozone, expressed as a percentage and ΔN the precision of the pair N-value (=0.41). The values in Table 3 lie between 0.7 and 1.4%.

g. Aerosols

A study of the effect of aerosols on the BUV total ozone retrieval was made by Dave (1978). He used 23 aerosol models containing both tropospheric and stratospheric aerosols, several aerosol size distributions and indices of refraction. The aerosol optical thicknesses at 312.5 nm range from 0.003 to 0.058 for the stratospheric aerosols models and from 0.193 to 1.033 for the tropospheric aerosols models (at the other BUV wavelengths the values are slightly larger). For the models containing both tropospheric and stratospheric components, the aerosol optical thickness are ~1.00. Some of the models contained large imaginary parts of the refractive index and hence had large absorption optical thicknesses.

For all cases examined, the error in the total O_3

was found to be less than 1% for all solar zenith angles <85.7°, even though the presence of aerosols had a significant effect on the backscattered radiance. For example, for the highest density purely scattering aerosol model at $\theta_0 = 60°$, an effective surface reflectivity of 21% was observed for a situation where the underlying surface reflectivity was 10%.

The contribution of the aerosol distributions studied to the total O_3 error budget is negligible. The effect of volcanic injection of aerosols has not been studied.

h. Radiative transfer computations

Dave's auxiliary equation solution to the radiative transfer equation (Section 3) is used to generate the standard radiance tables. Six iterations of the auxiliary equations are made. Each iteration accounts for the contribution due to one higher order of scattering. Multiple scattering is accounted for to better than 0.2% in all cases. A spherical shell correction is made to the incident radiation and residual spherical atmosphere effects are negligible in the angular range ($0 \leq \theta_0 \leq 85.7°$) of the total O_3 retrieval. Depolarization due to anisotropic scattering is accounted for in the scattering phase matrix and contributes no more than a fraction of a percent error in the computed radiances. Finally, interpolation of the standard tables is accurate to better than 0.1%. In all, the generation and interpolation of the standard radiances contribute only very slightly to the inaccuracy of the ozone retrieval.

i. Air scattering coefficients

The air scattering coefficients are well known and do not introduce any measureable error in the algorithm. Band effective scattering coefficients are averaged using the instrument response function and the wavelength-dependent scattering coefficients of Penndorf (1957). Perhaps the greatest uncertainty in the scattering coefficients is the depolarization factor which has the effect of increasing the total scattering cross section over that associated with the isotropic Rayleigh scattering. Raman scattering may be responsible for half of the observed depolarization (Hoyt, 1977). The depolarization factor used in Penndorf's computation accounts for the Raman scattering contribution to the total air scattering in an approximate way. The depolarization factors as measured by several experimenters (see Penndorf 1957, Table II) are consistent to ~10%. This means that the scattering coefficients are accurate better than 1% and introduce negligible errors with the total ozone retrieval.

j. Errors at large solar zenith angles

There are several errors which become important at solar zenith angles >77°. By far the most important error for BUV is the error due to the assumed vertical ozone distribution. Most of the discussion in this section will be concerned with these vertical profile errors. Of lesser importance are the errors due to the error in the solar zenith angle used in the retrieval, and the spherical atmosphere effects on the multiple scattered radiation.

A small error in the solar zenith angle at large values of solar zenith angle propagates into significant errors in the slant path length through the atmosphere, since this path is proportional to $\sec\theta_0$. Below 80°, the errors due to a 0.5° solar zenith angle error are just a small fraction of a percent. Near $\theta_0 = 85°$, the errors in ozone due to a 0.5° error in the solar zenith angle are ~2%. However, such large errors in the solar zenith angle are unlikely.

The spherical atmosphere is approximately accounted for as discussed earlier. Only multiple scattered radiation is not exactly corrected for spherical atmosphere attenuation. The attenuation of radiation between scatterings is computed based on a parallel plane geometry and the difference from the true spherical geometry is very small since the multiple scattering occurs in a relatively narrow layer of the atmosphere. The importance of this lower order spherical atmosphere effect is further minimized at large solar zenith angles, since the multiple scattering contribution becomes a smaller fraction of the total signal.

The algorithm sensitivity to profile shape becomes strong at large solar zenith angles. The increased absorption along the slant path of the incoming solar radiation prohibits the shorter wavelength radiation from penetrating to the surface. For this reason, the A-pair is more sensitive to the profile shape than is the B-pair.

The error in total O_3 due to profile shape depends on how the profile shape differs from the standard profile and on the sensitivity of the backscattered radiances to the profile shape differences. In general, the sensitivity will depend on the total O_3, the solar zenith angle, the surface reflectivity, the wavelength pair, and the region of the atmosphere when the profile shape is different from the standard profile shape.

Profile shapes errors were studied by simulating total O_3 retrievals for hundreds of O_3 profiles obtained from balloon measurements. In Fig. 4, the uncertainty in total ozone due to profile shape variations is plotted versus solar zenith for both the A- and B-pairs and for surface reflectivities of zero and one. The scale division for the solar zenith angle scale in this figure is based on a secant function in order to expand the high solar zenith angle behavior. The plotted uncertainty is based on 207 balloon profiles from Payerne and Hohenpeissenberg, having total ozone amount between 0.325 and 0.375 m-atm-cm. It can be seen that for low reflectivity, the A-pair total ozone estimate reaches an error of 3% at a solar zenith angle

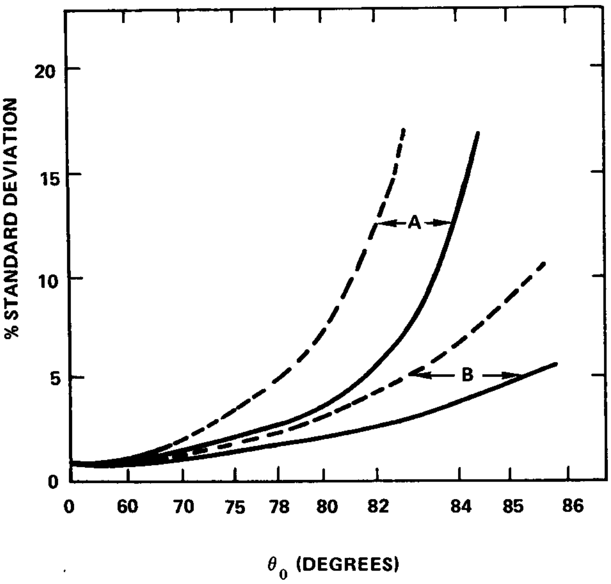

FIG. 4. Uncertainty in the A- and B-pair total ozone for $R = 0$ (dashed curves) and $R = 1$ (solid curves) plotted versus solar zenith angle.

of 75° and that the error increases rapidly beyond that point. The B-pair low reflectivity grows more slowly, reaching a 3% error at an angle of 82° and is only ~10%, even when the sun is within 4.3° of the horizon. The errors are much smaller for bright scenes which is an important advantage for BUV. The Nimbus-4 satellite was in a sun-sychronons orbit with equator crossing at local noon. Consequently, high solar zenith angles occur at high latitudes where scene reflectivities are usually high due to the presence of snow and increased cloudiness. Therefore, on the average, BUV errors are likely to fall between the two reflectivity curves for the B-pair in Fig. 4.

k. *Effective surface pressure*

The surface pressure for a clear scene is accurately determined using terrain height tables. Small errors in terrain pressure of ±0.025 atm are possible due to atmospheric pressure variation and interpolation of the terrain height tables. This leads to a very small error in the derived total O_3. For example, for $\theta_0 = 0°$, $\Omega = 0.35$ atm-cm and $R = 0$, an error of ±0.001 atm-cm would result. At 71.1°, $R = 0$ and $\Omega = 0.35$ atm-cm, the error is ±0.002 atm-cm. (If the B-pair were used at small values of θ_0, larger errors would result. This is one of the reasons why we chose the A-pair for low θ_0.)

For cloudy scenes, the error in the pressure of the cloud top causes a small error in the total O_3 retrieval. At reflectivities typical of full cloud cover ($R \approx 0.6$), the photometer N-value is almost completely independent of the surface pressure. Thus, the effective reflectivity is not in error. The error in total O_3 arises due to using the incorrect pressure tables for the pair N-values. If the cloud top pressure is overestimated by 100 mb, the total O_3 will be underestimated by ~1% at $\theta_0 = 0°$ and by 0.5% at $\theta_0 = 71.1°$.

5. Error summary

The errors discussed in the previous section are summarized in Table 4. The errors are grouped into two categories—systematic and random. Within the systematic category, we have sub-classified the errors according to three major sources—the measurement, the external information, and the algorithm and models used. Within the random error category, we distinguish between the measurement precision and algorithm precision. The algorithm precision is that caused by real physical random variations not modeled by the algorithm, e.g., tropospheric ozone variability.

Our overall accuracy estimate is 8–10%. This includes 6% due to the O_3 absorption coefficient, 1% due to measurement accuracy and 1–3% algorithm errors. At larger solar zenith angles, the accuracy estimate degrades to approximately 12% at 85.7° over dark surfaces.

For large data samples, the variations of the real atmosphere about the model atmosphere used in the algorithm resemble a random error. Errors such as tropospheric ozone variability, cloudiness, aerosols and profile shape errors at large solar zenith angles contribute. This pseudo-random component can be considered a kind of algorithmic precision. For clear sky, low to moderate solar zenith angles in the middle and high latitudes, this precision is 1.5%. For cloudy scenes and low to moderate solar zenith angles, the algorithm precision is 3%. The measurement precision is limited by the data word size of the measured radiance. The Nimbus 4 BUV precision is 0.7–1.3% depending on solar zenith angle. (For Nimbus 7 SBUV, this error is less than 0.1%.) The total overall precision is a combination (sum of squares) of the measurement and algorithmic precision which ranges from 1.7 to 3.4% for clear to fully cloudy situations. For low latitudes where the variability of the tropospheric ozone is small, the precision approaches the measurement precision 1.3% (from Table 3).

6. Observed errors

A degree of confidence in the error analysis discussed in the preceding sections can be obtained by studying the consistency of the A-pair and B-pair results and by comparing BUV results with the Dobson ground-station network. The observed errors are summarized in Table 5.

TABLE 4. Total ozone error summary for Nimbus-4 BUV.

		Systematic component			Random component	
Error	Description	Measurements	External information	Algorithm/ model	Measurements precision	Algorithm precision
Ozone absorption coefficients	(a) Absolute accuracy in 300 nm region	—	6%	—	—	—
Tropospheric ozone variability	Based on 50% variability					
	(a) Over dark or bright surface ($R < 0.2$, $R > 0.8$)	—	—	—	—	1½%
	(b) Over cloud	—	—	—	—	3%
Tropospheric ozone climatology	Based on 50% underestimate					
	(a) Dark ($R < 0.2$) 1.0 atm surface	—	—	−1½%	—	—
	(b) Bright ($R > 0.8$) 1.0 atm surface (does not exist in low latitude)	—	—	+1½%	—	—
	(c) Cloud top at 0.4 atm	—	—	3%	—	—
Bright snow/ice surface	(a) Middle latitudes (<55°)	—	—	3%	—	—
	(b) High latitudes (>55°) errors	—	—	<1%		
Instrument calibration	Absolute calibration via R	<1%	—	—	—	—
	Relative calibration	1%	—	—	—	—
Measurement noise	Data word size	—	—	—	0.7–1.3%	—
Aerosols	Based on Dave (1978) calculations	—	—	Extreme cases up to 1%	—	<0.5%
Radiative transfer computations	High-order multiple scattering	—	—	0.2%	—	—
	Table interpolation	—	—	0.1%	—	—
Scattering cross sections	Uncertainty in depolarization/ approximate accounting of Raman scattering	—	—	Less than 1%	—	—
Ozone profile shape Variability of large-solar zenith angle	(77° to 85.7°) Low reflectivity	—	—	up to 5%	—	3–10%
	High reflectivity	—	—	up to 3%	—	2–5%
Surface pressure errors	Terrain pressure precision ±25 mb	—	—	—	—	<0.5%
	For cloud top Variability ±100 mb Full Cloud $R = 0.6$	—	—	—	—	±½–1%

a. Bias

The BUV and Dobson results differ on the average by 3.5% and the BUV A-pair and B-pair results differ by 3.5%. It is likely that these differences are mainly due to differences in the O_3 absorption coefficients used.

b. Precision

The standard deviation of the Dobson/BUV difference is dependent on the measurement precision of both instruments, the precision of the BUV and Dobson algorithms and coincidence noise. The combined measurement and algorithmic precision of a

TABLE 5. Observed errors in total ozone from Nimbus 4 BUV.

	Accuracy	Precision
Dobson comparison		
Clear sky/AD-pair results Dobson-BUV	3.5%	—
Equatorial comparisons to minimize coincidence noise	—	1.0–1.5%
Overall precision Middle latitude–all codes	—	2.0–2.5%
Drift versus time	0.3–0.7% per year	—
Internal BUV consistency		
A-pair, B-pair difference		
Average	3.5%	—
Standard deviation	—	2–3%
A-pair, B-pair long-term drift	0.3–0.4% per year	—

well-operated Dobson instrument is estimated to be 1.5% (NASA Reference Publication 1049, 1979). The coincidence noise can be minimized using low-latitude intercomparisons. The standard deviation of the BUV/Dobson difference at the latitude stations closest to the equator range from 1.5 to 3.0%. Using a Dobson precision of 1.5%, the BUV precision estimate is 0–2.6%. The 1.5% Dobson precision is probably too large. Reducing the Dobson precision by half to 0.7%, the BUV precision estimate is 1.3–2.9%. This result is in agreement with our estimate for low latitudes based on measurement precision only, −1.3%.

Middle-latitude Dobson/BUV comparisons at Arosa in autumn for all conditions leads to a precision estimate for BUV of 2.0–2.5%. This falls between the clear sky and cloudiness algorithmic-precision estimates of 1.7–3.4%.

Another check on the BUV precision is the standard deviation of the difference between the A-pair and B-pair. This quantity is a composite of the instrument noise and only a fraction of the algorithmic noise. For small and moderate solar zenith angles and for clear sky, the algorithmic error due to tropospheric ozone is nearly the same for the two pairs and so the standard deviation for the AB difference is expected to be due to mainly measurement noise. The standard deviation of the AB difference for small reflectivities ($R < 0.2$) and moderate solar zenith angles is found to be 2.0–2.5%. This is in agreement with the error predicted based on measurement precision alone, −2%.

c. Long-term trends

Fleig *et al.* (1981) showed that long-term trends exist in the average equatorial radiances. Using Umkehr comparisons, they showed that a significant amount, if not all of the trend, at the shorter wavelengths could be associated with BUV instrument change (Fleig *et al.*, 1980). The BUV total ozone also shows a long-term trend relative to the Dobson network. The BUV/Dobson bias, using the full Dobson network, decreases with time for the first five years of BUV operation. After 1975, there is a hint of an increase but the drop in BUV coverage and corresponding coincidence statistics make the determination of trend beyond 1975 difficult. We have studied the decreasing BUV trend relative to Dobson using all stations, selected sub-sets and individual stations with good reputations. All of these analyses resulted in BUV decreasing trends, relative to Dobson, of between 0.3 and 0.7% per year for the 1970–75 time period.

Supporting the hypothesis that BUV instrumental drift was responsible for the long-term BUV/Dobson drift, is the relative A-pair/B-pair drift. For the full seven years of operation, the AB difference decreased almost linearly at a rate of 0.3–0.4% per year. It is likely that both the A-pair and B-pair are drifting and in the same direction. The drift of the difference can be considered an estimate of the minimum rate that the BUV total ozone has drifted. This is not necessarily the case if the drift is due to a slow change in the wavelength calibration. However, the on-board wavelength calibration measurement showed no sign of drifting.

7. Applicability to Nimbus 7 SBUV/TOMS ozone measurements

The Nimbus 7 SBUV and TOMS experiments also have the capability for total ozone determination. The algorithms for these experiments are improved versions of the algorithm described here, and differ in several significant ways. Therefore, we caution users who would use both data sets in their research that the two data sets are not entirely compatible. The SBUV/TOMS algorithms differ from the BUV algorithm in several ways: 1) use of the ozone absorption coefficients of Inn and Tanaka (1959) instead of Vigroux (1953); 2) use of a latitude-dependent cloud-top height climatology based on the Temperature and Humidity Infrared Radiometer (THIR) derived cloud parameters, replacing the 0.4 atm cloud height used by the Nimbus 4 BUV algorithm; 3) use of daily snow/ice maps; and 4) use of an improved retrieval scheme at high solar zenith angles. This list is not complete but mentions the major differences. Each of these modifications could cause a systematic difference between the data sets, however small. The differences are not easily determined or specified, since they will be complex functions of solar zenith angle, ozone, latitude, wavelength and reflectivity.

8. Summary

The precision of the BUV total ozone retrieval is better than 2% for ideal clear sky conditions which occur nearly 50% of the time. The precision is better than 4% for most other conditions. Retrievals at solar zenith angles between 82–86° are better than 5%, but comprise only a few percent of the data set. Overall, the precision of the global data set is ~3%.

The BUV data set is a high-quality, independent, global and multi-year data set. The ozone data are archived at the World Data Center-A for rockets and satellites. These data sets can be obtained from the National Space Science Data Center, NASA, Goddard Space Flight Center, Greenbelt, MD.

Acknowledgments. We would like to thank Drs. Carlton Mateer of the Canadian Atmospheric Environment Service, Donald Heath of NASA Goddard Space Flight Center and J. V. Dave of the IBM Corporation for their invaluable advice and support in the development of this algorithm. We also acknowledge helpful discussions with Dr. R. Fraser, Dr. J. Gatlin, Mr. E. Hilsenrath and Dr. B. Guenther. The contribution to this work by Systems and Applied Sciences Corporation was made under contract to the National Aeronautics and Space Administration under Contracts NAS5-24416, NAS5-25346 and NAS5-26753.

REFERENCES

Attmannspacher, W., and R. Hartmannsgruber, 1980: Trend and extreme values of 8 years of continuous measurements of ozone near the surface at the Meteorological Observatory Hohenpeissenberg, FRG. *Proc. Quadrennial Int. Ozone Symp.*, Boulder, International Ozone Commission, 492–497.

COESA, 1976: *U.S. Standard Atmosphere.* U.S. Government Printing Office, Washington, DC.

Dave, J. V., 1964: Meaning of successive iteration of the auxiliary equation in the theory of radiative transfer. *Astrophys. J.*, **140**, 1292–1303.

——, and C. L. Mateer, 1967: A preliminary study on the possibility of estimating total atmospheric ozone from satellite measurements. *J. Atmos. Sci.*, **24**, 414–427.

——, 1978: Effect of aerosols on the estimation of total ozone in an atmospheric column from the measurement of its ultraviolet radiance. *J. Atmos. Sci.*, **35**, 899–911.

DeLuisi, J. J., and C. L. Mateer, 1971: On the application of the optimum statistical inversion technique to the evaluation of umkehr observations. *J. Appl. Meteor.*, **10**, 328–334.

——, 1975: Measurements of the extraterrestrial solar radiant flux from 2981 to 4000 Å and its transmission through the earth's atmosphere as it is affected by dust and ozone. *J. Geophys. Res.*, **80**, 345–354.

Dobson, G. M. B., 1963: Note on the measurement of ozone in the atmosphere. *Quart. J. Roy. Meteor. Soc.*, **89**, 409–411.

Fleig, A. J., V. G. Kaveeshwar, K. F. Klenk, M. R. Hinman, P. K. Bhartia and P. M. Smith, 1980: Characteristics of space and ground based total ozone observing systems investigated by intercomparison of Nimbus-4 Backscattered Ultraviolet (BUV) data with Dobson and M83 results. *Proc. Quadrennial Int. Ozone Symp.*, Boulder, International Ozone Commission, 9–16.

——, K. F. Klenk, P. K. Bhartia, K. D. Lee, C. G. Wellemeyer and V. G. Kaveeshwar, 1981: Vertical ozone profile results from the Nimbus-4 BUV data. *Preprints, Fourth Conf. Atmospheric Radiation*, Toronto, Amer. Meteor. Soc., 20–26.

Fraser, R. S., and Z. Ahmad, 1978: The effect of surface reflection and clouds on the estimation of total ozone from satellite measurements. *Fourth NASA Weather and Climate Program Science Review*, E. R. Kreins, Ed., NASA Conf. Publ. 2076, 247–252. [NTIS N7920633].

——, and ——, 1978: The effect of anisotropic surface reflection on the accuracy of total ozone estimates from satellite observations. *Preprints, Third Conf. Atmospheric Radiation*, Davis, Amer. Meteor. Soc., 63–66.

Heath, D. F., A. J. Krueger and C. L. Mateer, 1970: *Nimbus 4 User's Guide*, R. R. Sabatini, Ed. Goddard Space Flight Center, Greenbelt.

Hoyt, D. V., 1977: A redetermination of the Rayleigh optical depth and its application to selected solar radiation problems. *J. Appl. Meteor.*, **16**, 432–436.

Inn, E. C. Y., and Y. Tanaka, 1959: *Ozone Chemistry and Technology.* ACS Appl. Publ., Amer. Chem. Soc., Washington, DC, 263–268.

Kirchhoff, V. W. J. H., Y. Sahai and A. G. Motta, 1981: First ozone results measured with ECC sondes at Natal (5.9°; 35.2°W). *Geophys. Res. Lett.*, **8**, 1171–1172.

Klenk, K. F., 1980: Absorption coefficients of ozone for the backscatter UV experiment. *Appl. Opt.*, **19**, 236–242.

Komhyr, W. D., 1980: Dobson spectrophotometer systematic total ozone measurement error. *Geophys. Res. Lett.*, **7**, 161–163.

Krueger, A. J., and R. Minzner, 1976: A midlatitude ozone model for the 1976 U.S. Standard Atmosphere. *J. Geophys. Res.*, **81**, 4477–4481.

McPeters, R. D., and A. M. Bass, 1982: Anomalous atmospheric spectral features between 300 and 310 nm interpreted in light of new ozone absorption coefficient measurements. *Geophys. Res. Lett.*, **9**, 227–230.

Mateer, C. L., and H. U. Dutsch, 1964: Uniform evaluation of umkehr observations from the world ozone network, Part I. NCAR, Boulder, 20 pp.

——, D. F. Heath and A. J. Krueger, 1971: Estimation of total ozone from satellite measurements of backscattered ultraviolet earth radiance. *J. Atmos. Sci.*, **28**, 1307–1311.

NASA Reference Publication 1049, 1979: *The Stratosphere: Present and Future.* R. Hudson and E. Reed, Eds., 286 pp. [NTIS N8014641].

Penndorf, R., 1957: Tables of the refractive index for standard air and the Rayleigh scattering coefficient for the spectral region between 0.2 and 20.0 μ and their application to atmospheric optics. *J. Opt. Soc. Amer.*, **47**, 176–182.

Vigroux, E., 1953: Contribution a l'étude experimentale de l'absorption de l'ozone. *Ann. Phys.*, **8**, 709–762.